CHARLES ELACHI

SPACEBORNE IMAGING RADAR RESEARCH IN THE 1990s: AN OVERVIEW

Spaceborne imaging radar will be used in the 1990s for global surface observations, for intensive research on surface process, and to map the surface topography on a global basis.

INTRODUCTION

The imaging radar experiments on Seasat (1978) and on the space shuttles (SIR-A in 1981 and SIR-B in 1984) have resulted in wide interest in the use of spaceborne imaging radars in earth and planetary sciences. The radar sensors provide unique and complementary information about what is acquired with visible and infrared imagers, including subsurface imaging in arid regions,[1,2] all-weather observations of ocean-surface dynamic phenomena,[3-5] structural mapping,[6-8] soil moisture mapping,[9] and stereo imaging and the resulting topographic mapping.[10]

Until now, experiments have exploited only a very limited range of the generic capability of radar sensors. With planned sensor developments in the late 1980s and early 1990s, a quantum jump will be made in our ability to exploit fully the potential of these sensors. Developments include (Table 1) multiparameter research sensors such as SIR-C and X-SAR; long-term and global monitoring sensors such as the European ERS-1, the Japanese JERS-1, the Canadian Radarsat, and the proposed NASA programs EOS (Earth Observing System) and GLORI (Global Radar Imager), the spaceborne sounder; and planetary mapping sensors such as the Venus Magellan and Cassini/Titan mappers, topographic three-dimensional imagers such as the scanning radar altimeter, and three-dimensional rain mapping. These sensors and their associated research are briefly described in this article.

MULTIPARAMETER RESEARCH IMAGING RADAR: THE SIR PROJECT

An evolutionary 10-year program is under way at NASA's Jet Propulsion Laboratory to develop the scientific application and technological aspects of multiparameter imaging radars. The first two steps consisted of the SIR-A, which was a single-frequency proof-of-concept sensor, and the SIR-B, which was designed to acquire multiangle imagery. The SIR-A demonstrated the ability of spaceborne radars to acquire subsurface imagery in arid regions (Fig. 1). The SIR-B provided stereo imagery from space for the first time (Fig. 2). For recent results acquired with SIR-B, see Refs. 10 and 11.

The next major step in the SIR project is the joint United States/Germany/Italy SIR-C/X-SAR experiment, which will allow the simultaneous acquisition of images at three frequencies (L, C, and X bands) and at all polarization states (on the L and C channels). The multifrequency capability will allow the study of the surface spectral response and the classification of surface units based on the roughness and dielectric properties. It will also allow the quantitative determination of the subsurface penetration, which is a strong function of the frequency.

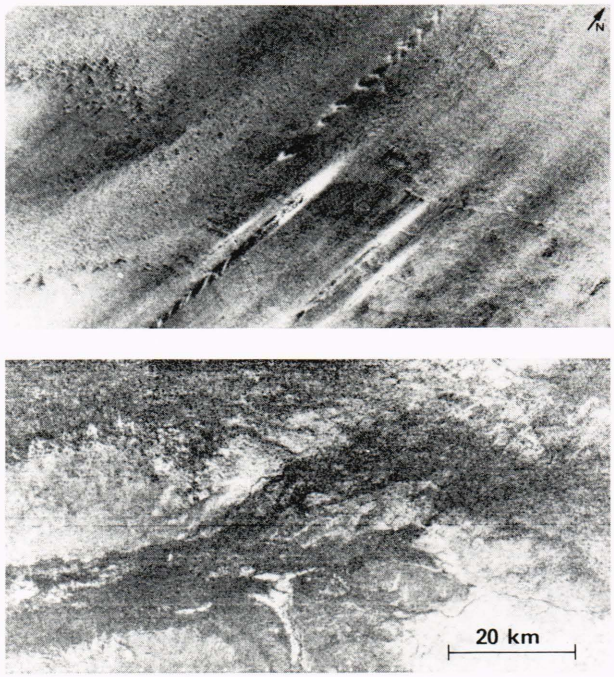

Figure 1—Landsat (top) and SIR-A (bottom) images of the same desert area in southwestern Egypt. The SIR-A clearly shows the morphology of dry river channels buried a few meters under a layer of dry sand.

Charles Elachi is a senior research scientist and manager of the Earth and Space Sciences Division, NASA/Jet Propulsion Laboratory, Pasadena, CA 91109.

Table 1—Spaceborne imaging radar sensors of the 1980s and 1990s.

Completed and ongoing elements of the NASA SIR core project

	SIR-A/B 1981/1984	*Airborne Facility 1987*	*SIR-C/D 1990, 1991, 1993*	*SIR-E (EOS) 1994–*
Frequency (GHz)	1.25 (L band)	1.25 (L band) 5.3 (C band)	1.25 (L band) 5.3 (C band) 9.6 (X band)*	1.25 (L band) 5.3 (C band) 9.6 (X band)*
Polarization	HH	HH,VV,HV,VH	HH,VV,HV,VH	HH,VV,HV,VH
Resolution (m)	20–40	10	10–60	10–20
Swath width (km)	30–50	10–20	15–80	50–300
Illumination control	Mechanical	N/A	Electronic	Electronic
Architecture	Conventional	Conventional	Distributed	Distributed *Germany/Italy

International free-flying sensors

	ESA/ERS-1 1990	*Japan/JERS-1 1991*	*Canada/Radarsat 1992*	*US/EOS 1994*
Frequency (GHz)	5.3	1.2	5.3	1.2 5.3 9.6*
Resolution (m)	30 or 100	18	28	10–20
Swath width (km)	80	75	130	50–300
Illumination angle	23°	42°	20–45°	10–55° (controllable)
Main thrust	Oceanography	Geology	Polar ice	Multidisciplinary *Germany/Italy

Nonconventional spaceborne imaging radar sensors being studied

Scanning radar altimeter 1992/1993	*Radar rain mapper 1988/1994*	*Global radar imager (GLORI) (1994)*	*Imaging sounder (1998)*
Global digital land topography	Three-dimensional precipitation mapping	Global coverage every two days	Subsurface sounding in arid regions and ice sheet
250 m spatial, 3 m height resolution	1 km spatial, 100 m height resolution	100 m spatial resolution	500 MHz (P band)
Two shuttle flight global coverage	150–300 km swath	700–800 km swath	
37 GHz	15/37 GHz	5.3 GHz (C band)	

The polarization capability will allow the synthesis of the surface images at all possible polarization states based on coherently acquiring the four fundamentals (HH, VV, HV, and VH), as shown in Fig. 3 and discussed in detail in Refs. 12 to 14.

The SIR project's activities also include major technological developments (including distributed synthetic aperture radar (SAR) and real-time ground data processing and calibration) that will form the basis for the EOS SAR.

LONG-TERM AND GLOBAL EARTH OBSERVATIONS

The SIR experiments will be limited to short-period 1-week flights until the EOS platform is orbited in the mid 1990s. In the meantime, a number of imaging radar

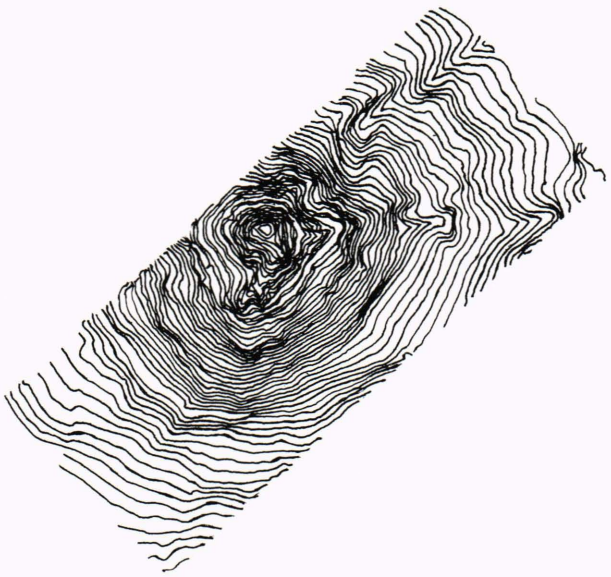

Figure 2—Stereo images acquired by the SIR-B were used to generate topographic contours (top) and perspective views (bottom) of Mt. Shasta in California.

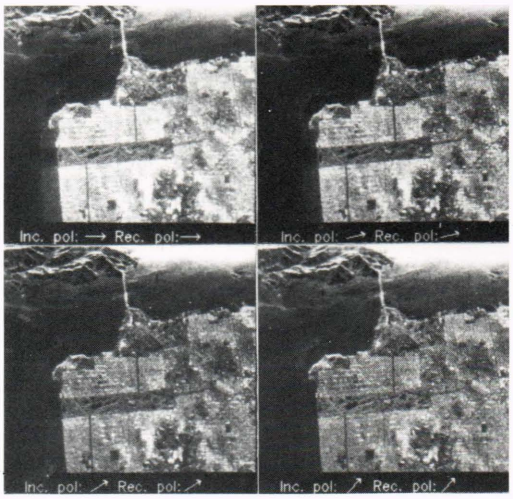

Figure 3—Synthesized polarization diversity images of San Francisco Bay generated from the four basic coherent images at HH, VV, VH, and HV polarization acquired with the JPL L-band airborne radar.

sensors are planned for launch on free flyers in the early 1990s for long-term surface observations. These sensors will have limited parameter flexibility but will play a major role in allowing the study of the temporal behavior of surface phenomena such as sea ice, ocean waves and patterns, vegetation dynamics, and forest clear cutting. The European ERS-1 and Japanese JERS-1 are approved projects that are planned for the early 1990s with lifetimes of 2 to 3 years. However, because of their limited swath (100 kilometers) and operation range (within view of a station), their monitoring capability will be localized. This led JPL scientists to the feasibility study of GLORI, which will allow global mapping every 2 days. GLORI requires a sensor with dual 400-kilometer swaths. The preliminary concept contains a C-band sensor with a 100-meter resolution and real-time processing on the EOS platform. Such a sensor will allow global and continuous monitoring of polar ice, large ocean phenomena (internal waves, eddies, weather fronts, and current boundaries), soil moisture, and vegetation cover.

Subsurface penetration is directly proportional to the observing radar wavelength; this led to the considerations of a low-frequency imaging SAR. Even though very low frequencies are desired, ionospheric effects and frequency allocation considerations will limit the lower transmitted frequency to about 400 megahertz. This would extend the penetration depth in arid regions observed by SIR-A by a factor of 3. In addition, such a sensor would allow the sounding of the Antarctic ice sheets down to a depth of many kilometers because of the extremely low loss properties of ice.

PLANETARY OBSERVATIONS

The cloud-penetration capability of radar sensors makes them a unique tool for imaging the surfaces of Venus and Titan, which are continuously and completely cloud covered. The Magellan mission will put an S-band imaging SAR in orbit around Venus in 1990 to provide images of at least 90 percent of the planet's surface at a resolution better than 250 meters. By the late 1990s, the Cassini spacecraft will be in orbit around Saturn, and, through a series of flybys, the surface of Titan will be imaged and sounded with a dual-frequency (L- and K-band) imaging radar sensor.

THREE-DIMENSIONAL IMAGING

Surface topography is a key database for fully interpreting the imaging data acquired with multispectral (microwave, infrared, and visible) sensors. When the topography is registered to the imaging data, the interpreter can use graphic techniques to observe the surface from a variety of perspective views (Fig. 4), thus enhancing his interpretation capability.

High-resolution topography can be derived from stereo imagery (radar or visible/infrared). However, this is practical only for regional coverage. The acquisition

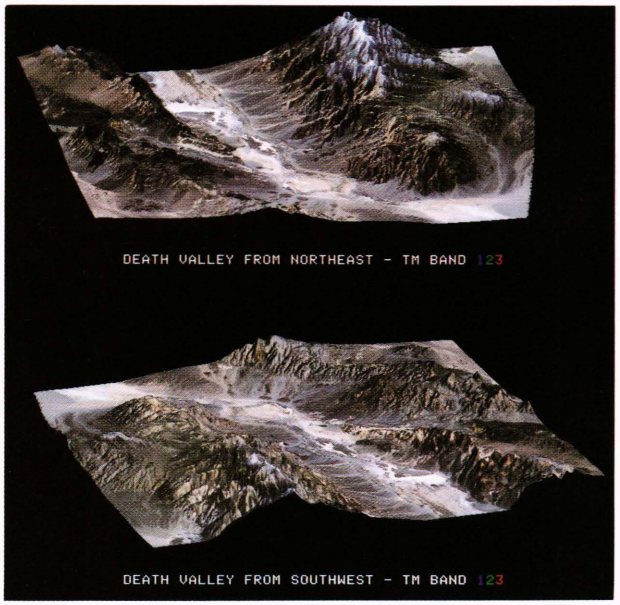

Figure 4—Perspective views of Death Valley, Calif., generated from thematic mapper data coregistered on a digital surface topography base.

of a global digital database at a reasonable cost and in a timely fashion requires the development of a technique that allows the direct measurement of the surface topography in a digital format; this can be done with a scanning radar altimeter (Fig. 5).

The scanning radar altimeter uses a narrowbeam antenna across the track with a surface footprint of 250 meters, which is possible with an 8-meter, 37-gigahertz antenna from an altitude of 250 kilometers. Along the track, a synthetic aperture technique is used to achieve the equivalent spatial resolution by means of an antenna of only 0.3 meter. The beam is scanned back and forth across the track to cover a 150-kilometer swath. In this configuration, two shuttle flights will be sufficient to acquire the global data sets. A height accuracy measurement of less than 3 meters is feasible.

The scanning radar altimeter concept can also be used for volumetric rain mapping. Figure 6 shows an example of rain profiles acquired with a downlooking airborne sensor.[13] The rain intensity can be derived for each altitude level, particularly if a dual-frequency sensor is used. By scanning back and forth, a three-dimensional "picture" of the rain region can be acquired.

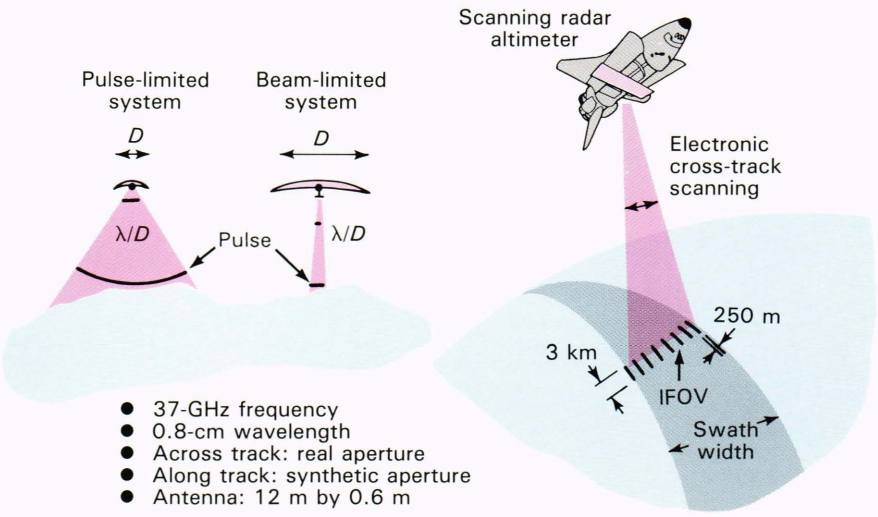

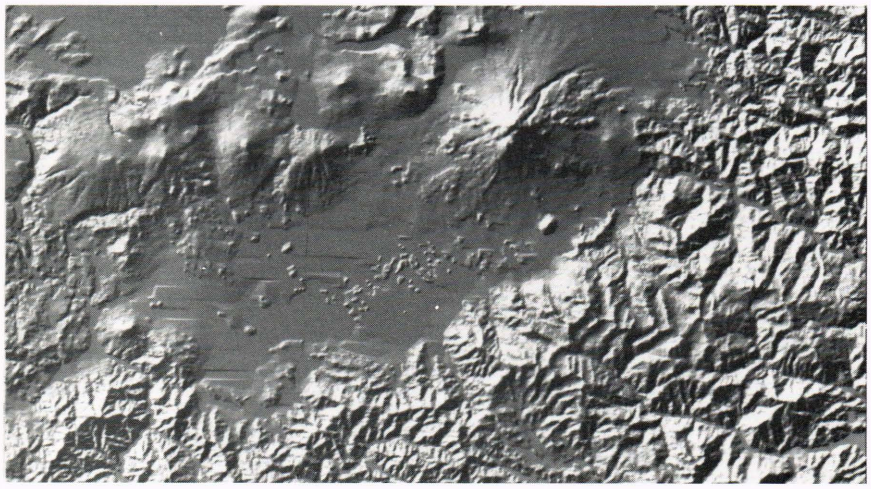

Figure 5—(a) Concept of a scanning imaging altimeter for global topographic mapping and (b) a shaded relief map of Mt. Shasta generated from a simulation of the data that will be provided by such a sensor.

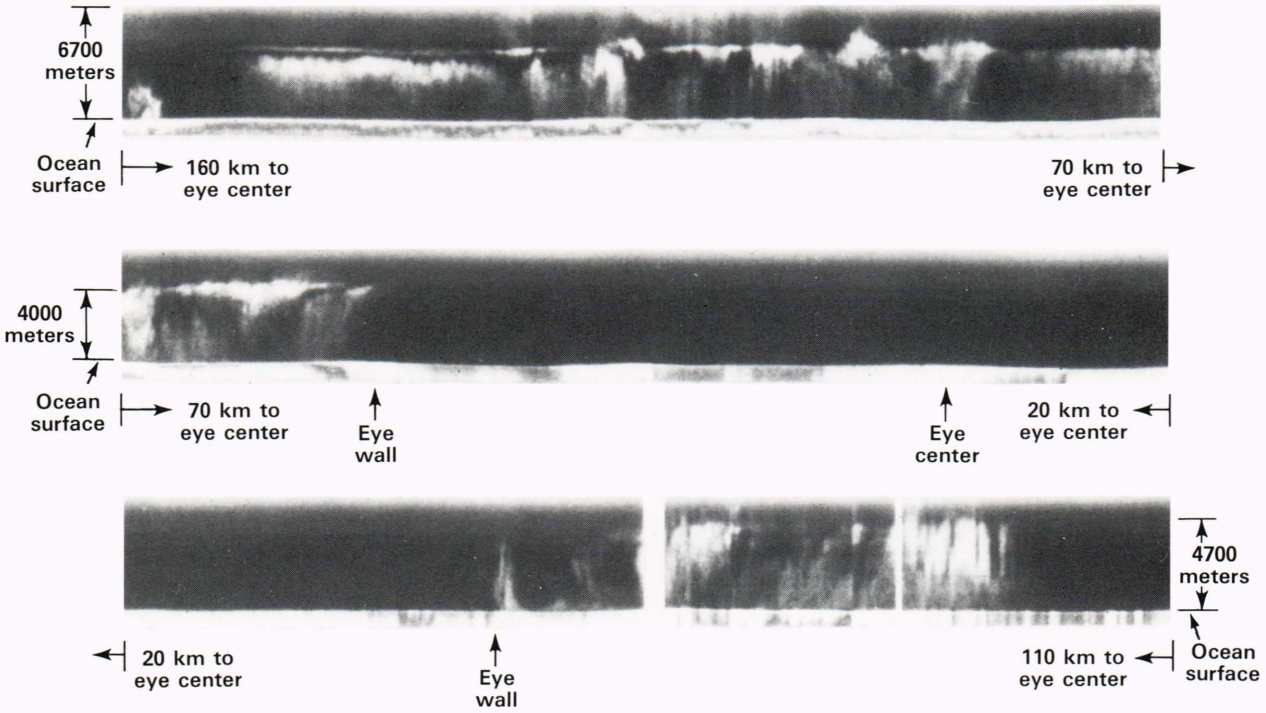

Figure 6—Concept of a scanning radar rain mapper and an example of airborne radar data showing rain images in one vertical plane.

CONCLUSION

This overview illustrates the wide range of experiments that are planned to capitalize on the capability of spaceborne radar sensors. It is important to note that in order to acquire a comprehensive information set about the surface, the radar data have to be used in conjunction with visible and infrared data. In this fashion, the user will be able to determine the surface composition (from visible and infrared spectrometry), its thermal properties (from thermal infrared), its physical and electric properties (from multispectral imaging radar), and its morphology (from stereo imagers or scanning altimeters).

REFERENCES

[1] J. McCauley et al., "Subsurface Valleys and Geoarcheology in the Eastern Sahara Revealed by Shuttle Radar," *Science* **218**, 1004 (1982).

[2] C. Elachi, L. Roth, and G. Schaber, "Spaceborne Radar Subsurface Imaging in Hyperarid Regions," *IEEE Trans. Geosci. Remote Sensing* **GE-22**, 383 (1984). (The SIR-A and Landsat images in Fig. 2 of this reference were mistakenly interchanged.)

[3] J. Vesecky and R. Stewart, "The Observation of Ocean Surface Phenomena Using Imagery from Seasat SAR," *J. Geophys. Res.* **87**, 3397 (1982).

[4] C. Elachi, "Spaceborne Imaging Radar: Geologic and Oceanographic Applications," *Science* **209**, 1073 (1980).

[5] C. Elachi, "Radar Imaging of the Ocean Surface," *Boundary-Layer Meteorol.* **13**, 165 (1978).

[6] F. F. Sabins, Jr., "Geologic Interpretation of Space Shuttle Radar Images of Indonesia," *AAPG Bull.* **67**, 2076 (1983).

[7] J. P. Ford, "Seasat Orbital Radar Imagery for Geologic Mapping: Tennessee-Kentucky-Virginia," *AAPG Bull.* **66**, 2064 (1980).

[8] F. F. Sabins, Jr., R. Blom, and C. Elachi, "Seasat Radar Image of the San Andreas Fault, California," *AAPG Bull.* **64**, 614 (1980).

[9] K. Carver, C. Elachi, and F. Ulaby, "Microwave Remote Sensing," *IEEE Proc.* **73**, 970 (1986).

[10] *Science* **232** (Jun 20, 1986).

[11] J. B. Cimino, C. Elachi, and M. Settle, "SIR-B – The Second Shuttle Imaging Radar Experiment," *IEEE Trans. Geosci. Remote Sensing* **GE-24**, 445 (1986).

[12] D. Evans, T. Farr, J. P. Ford, T. Thompson, and C. Werner, "Multi-Polarization Radar Images for Geologic Mapping and Vegetation Discrimination," *IEEE Trans. Geosci. Remote Sensing* **GE-24**, 246 (1986).

[13] J. Van Zyl, H. Zebker, and C. Elachi, "Theory of Imaging Radar Polarimetry through Wave Synthesis" (submitted to *Radio Sci.*, 1986).

[14] H. Zebker, J. Van Zyl, and D. Held, "Imaging Radar Polarimetry from Wave Synthesis" (submitted to *J. Geophys. Res.*, 1986).